# Supporting Information for Confined-but-Connected Quantum Solids Via Controlled Ligand Displacement

*William J. Baumgardner*[†], *Kevin Whitham*[‡], *Tobias Hanrath*[§]

[†]Department of Chemistry and Chemical Biology, Cornell University, Ithaca, NY 14850

[‡]Department of Materials Science and Engineering, Cornell University, Ithaca, NY 14850

[§]School of Chemical and Biomolecular Engineering, Cornell University, Ithaca, NY 14850

## Materials

Lead oxide (99.99%), selenium (99.999%, powder), trioctylphosphine (90%, technical grade), oleic acid (70%, technical grade), diphenylphosphine (98%), toluene (99.8%, anhydrous), N-N dimethylformamide (99.8% anhydrous), methylformamide (98%),2-dimethylaminoenthanol (98%, purum), ethanol (99.5%, anhydrous), methanol (99.8%, anhydrous), diethylene glycol (99%), acetone (99.8%), and acetonitrile (99.8%, anhydrous) were all purchased from Sigma Aldrich and used without purification. Deionized water was obtained from a lab installed deionizer.

## Solubility Study

The solubility of OA in DMAE, DEG, and MF were not readily available in the literature. To determine the relative solubility of OA in these solvents, we added OA (50% by volume) to each and found that DEG and DMAE formed a miscible solution while MF caused OA to crystallize and precipitate after a few hours, indicating limited OA solubility.

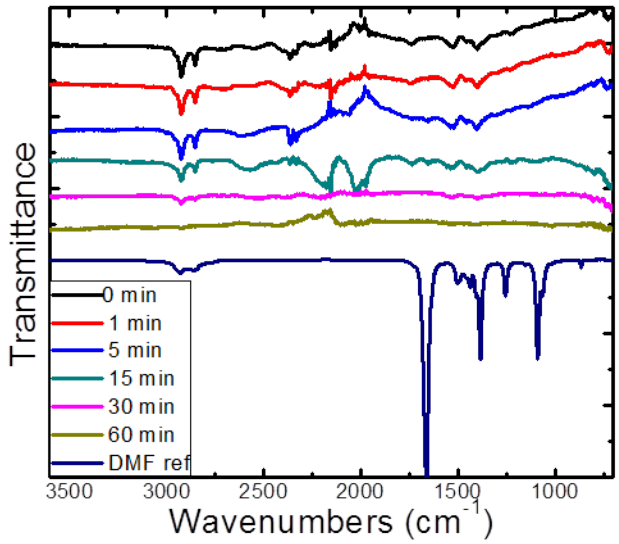


**Figure S1.** Fourier transform infrared spectroscopy of a film of spincoated 6.7 nm PbSe QDs as a function of DMF treatment time.

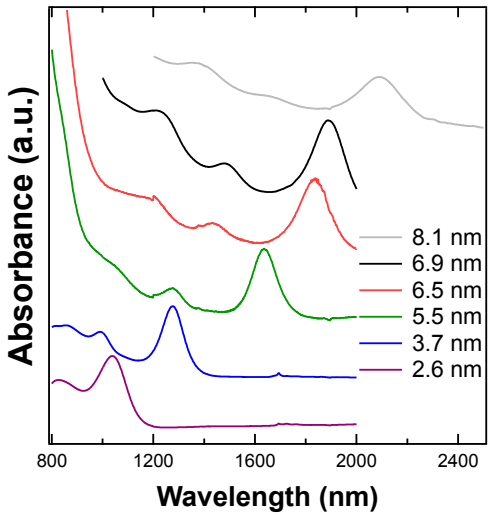


**Figure S2.** Absorbance spectra for PbSe QDs from 2.6 nm to 8.1 nm.

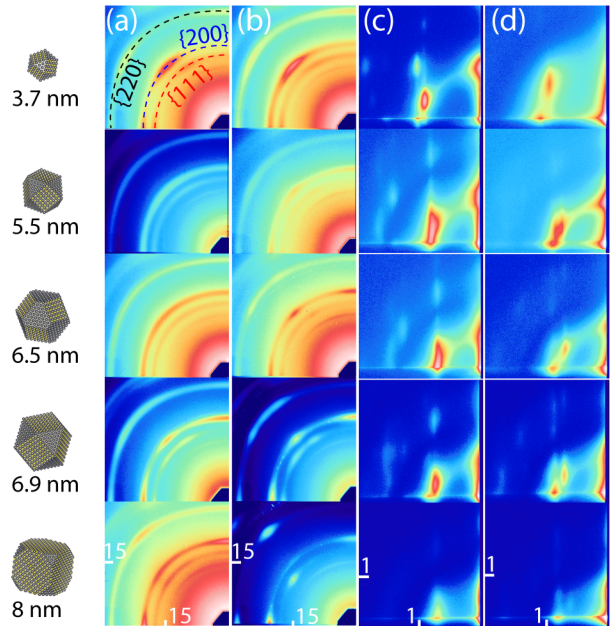


**Figure S3.** Diffraction patterns of PbSe QD films by GIWAXS (a,b) and GISAXS (c,d) for a range of QD diameters. Untreated samples (c) show BCC (3.7 nm, 6.9 nm) or FCC (5.5 nm, 6.5 nm) superlattice symmetry. FCC symmetry is accompanied by random QD orientation (a). Samples immersed in DMF for 50 minutes show BCC symmetry (d) and orientational alignment (b). The scale of the in-plane and out-of-plane reflections is shown in the bottom row, units are $nm^{-1}$.

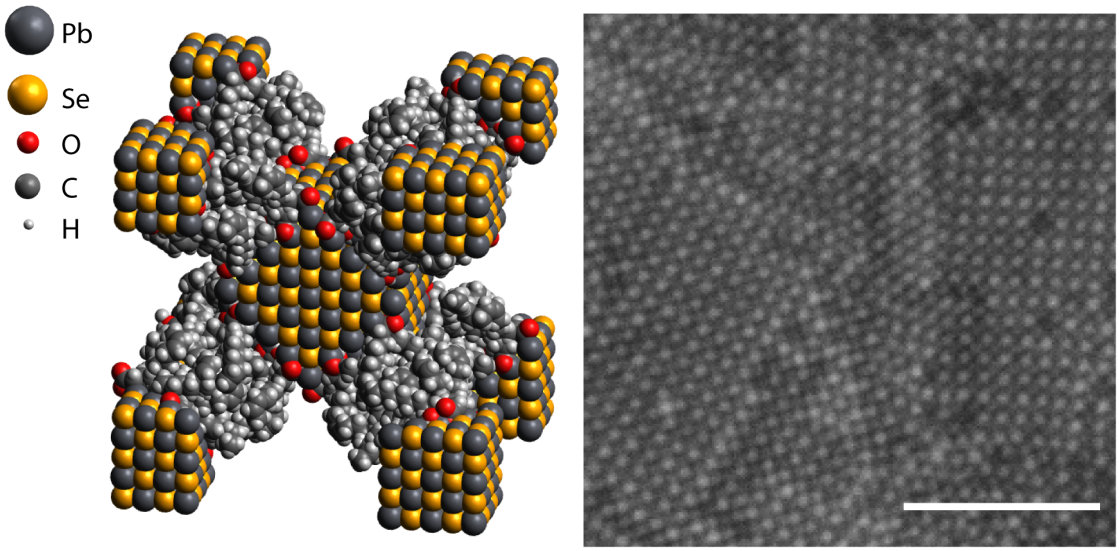


**Figure S4.** On left, a unit cell of the superlattice structure formed by 3.7 nm PbSe QDs measured by GISAXS and GIWAXS, showing the eight-fold coordination of the BCC structure. Oleic acid molecules decorate the {111} facets. On right is an SEM micrograph showing the (001) plane of a BCC superlattice formed by untreated spin-cast 6.9 nm PbSe QDs, scale bar is 100 nm.

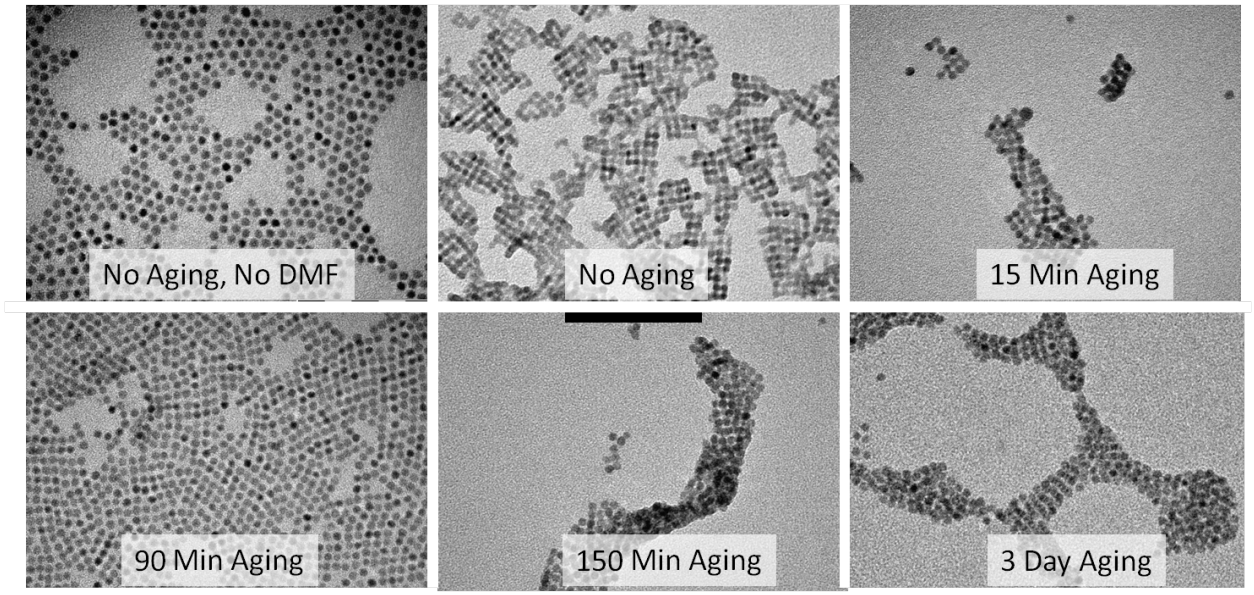


**Figure S5.** TEM images of 6.7 nm PbSe QD films a function of aging time prior to DMF treatment. Except the image in the upper left, all films were soaked in pure DMF for 15 minutes prior to imaging. The aging time refers to the time the PbSe QDs were in atmosphere before being cast onto the TEM grid. Scale bar represents 200 nm.

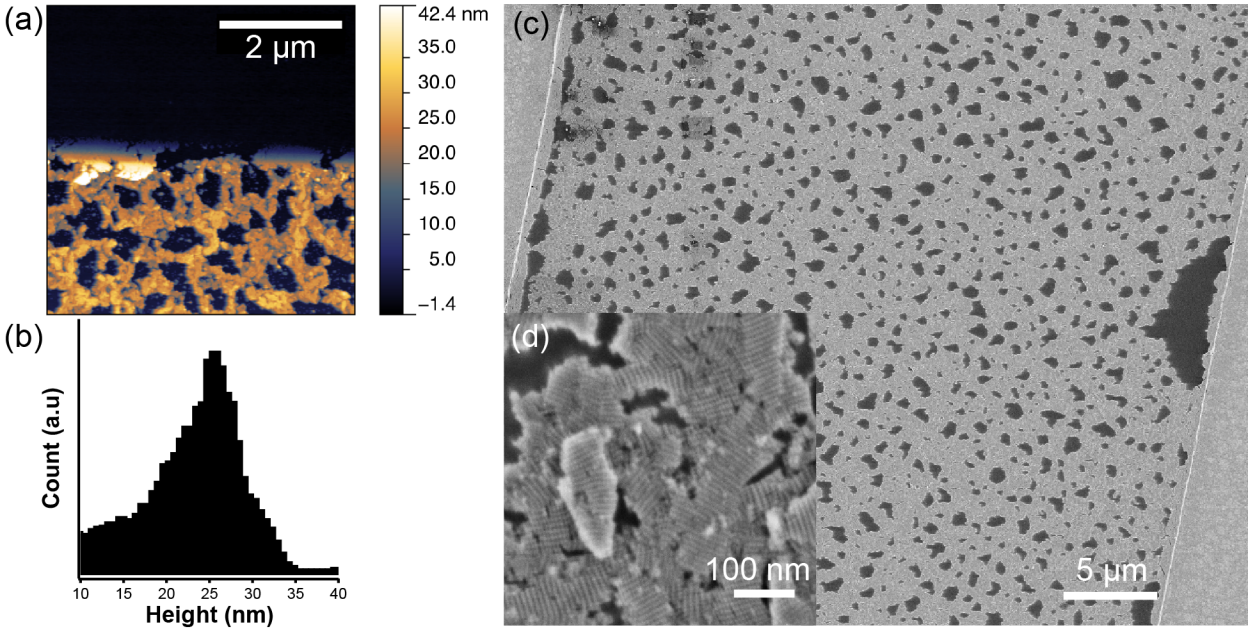


**Figure S6.** Characterization of a spin cast film of 6.7 nm PbSe QDs treated with DMF and used for conductivity measurement. A histogram (b) of the height data measured by AFM in (a) shows an average thickness of 25 nm. SEM image (c) showing Au electrodes at left and right. Higher magnification image of the film (d) shows superlattice domains of tens to hundreds of nanometers.

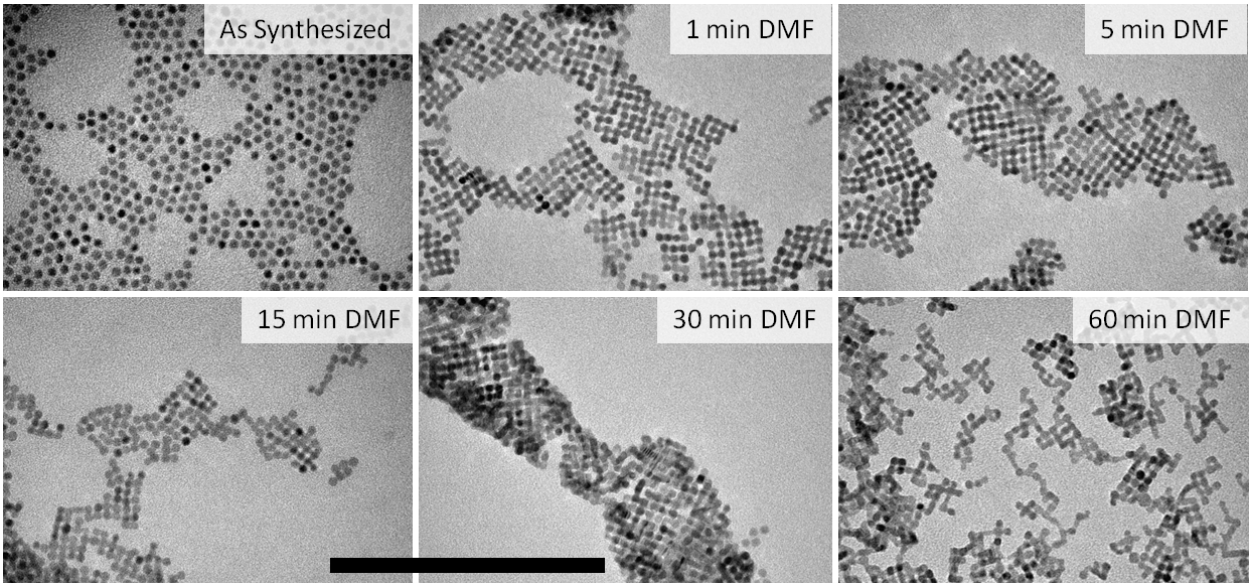


**Figure S7a.** TEM images of 6.7 nm PbSe QD films treated with DMF for varying lengths of time. None of these films had been exposed to air prior to treatment. Scale bar represents 200 nm.

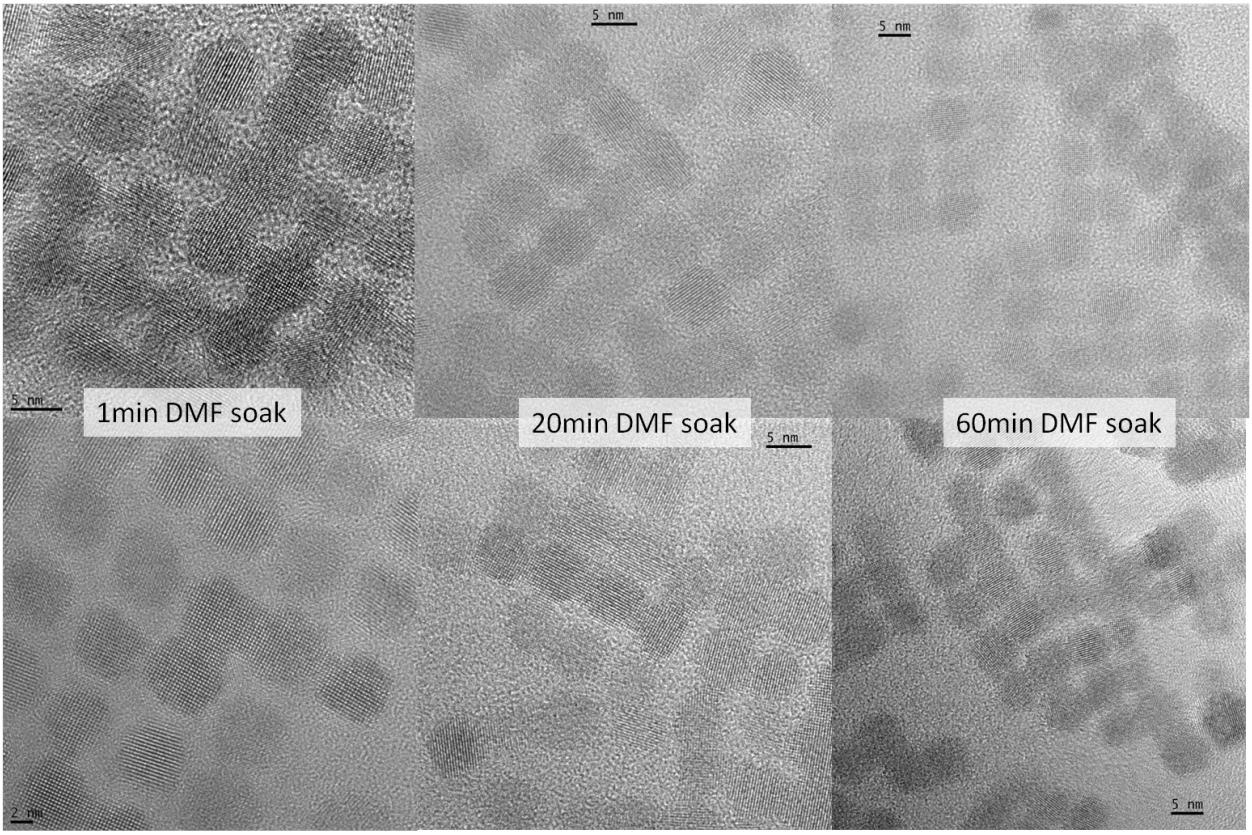


**Figure S7b.** High resolution TEM images of 6.7 nm PbSe NCS after treatment for 1 min, 20 min, and 60 min with DMF.

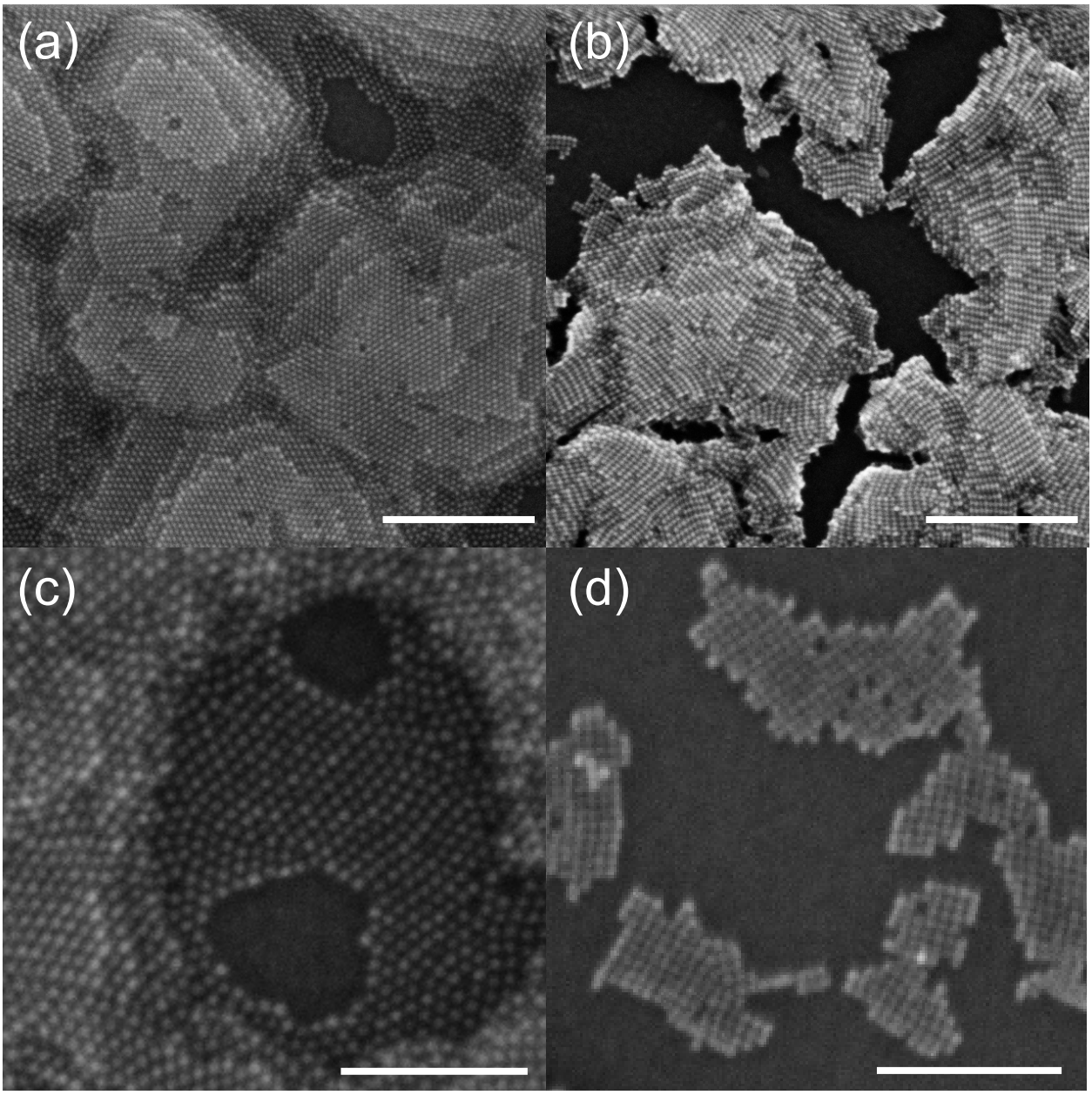


**Figure S8.** Scanning electron micrographs of 6.9 nm diameter PbSe QDs before (a,c) and after (b,d) treatment with DMF for 60 minutes. Scale bars are 200 nm.

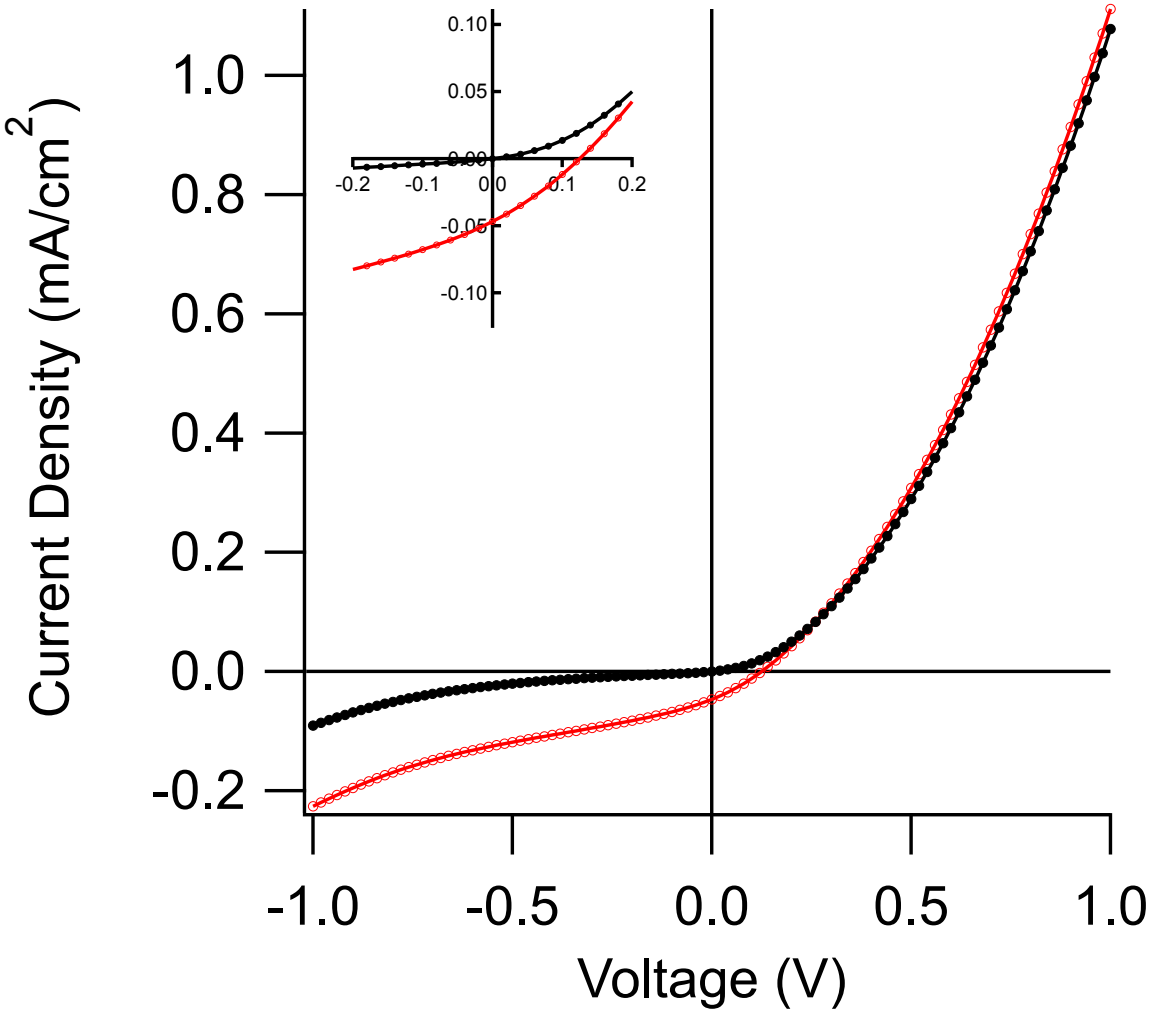


**Figure S9.** Current-voltage response of a photovoltaic device fabricated with 3.6 nm diameter PbSe QDs treated with DMF. Black curve with closed circles was measured in the dark, red curve with open circles was measured under 40 W/m$^2$ white light. The inset shows a scaled representation of the data to highlight short-circuit current at 0.05 mA/cm$^2$ and open-circuit voltage at 0.12 V.